



MODELING AND ANALYSIS OF MEDIA INFLUENCE OF INFORMATION DIFFUSION ON THE SPREAD OF CORONA VIRUS PANDEMIC DISEASE (COVID-19)

Fekadu Tadege Kobe¹, Lipon Chandra Das^{2*}, A. S. M. Mohiul Islam³, Anisul Islam⁴,
Sujit Kumar Roy⁵

Abstract

The article presents a deterministic mathematical model to analyze the impact of media outreach influence of information diffusion on the spread of the COVID-19 pandemic disease. The model consists of seven non-linear differential equations that describe the impact of awareness programs on the spread of COVID-19. Pandemic diseases such as influenza have been proposed and analyzed in the context of the impact of awareness programs on the spread of the respective diseases. The growth rate of educational efforts is proportional to the number of infected individuals, and susceptible individuals form a separate class, influenced by their environment, avoid contact with infectious ones. The stability theory of differential equations is employed to analyze the model. It reveals that while awareness programs control COVID-19 spread, immigration sustains its pandemic status. Models were qualitatively analyzed to determine criteria for controlling the spread of COVID-19 and to calculate baseline reproduction and equilibrium. However, a stable disease-free equilibrium coexists with a stable endemic equilibrium within a specific range of associated reproduction numbers below one. The analysis and modeling results propose that the most effective strategies for controlling or eradicating the COVID-19 pandemic involve utilizing information diffusion and media-influenced awareness programs. These approaches prove beneficial in reducing disease spread by effectively separating susceptible individuals from infectious ones.

Key Words: modeling; information diffusion; media influence; Stability analysis; SEIR model; COVID-19

¹ College of Natural and Computational Science, Department of Mathematics, Wachemo University, Hossana, Ethiopia,

¹ Department of Applied Informatics and Probability Theory, Mathematics and Natural Sciences, Russian University of Friendship of Peoples, Russia

^{2, * 3} Department of Mathematics, University of Chittagong, Chittagong-4331, Bangladesh

⁴ Computer and Information Sciences, University of Northumbria at Newcastle, UK.

⁵ Institute of Water and Flood Management, Bangladesh University of Engineering and Technology, Bangladesh

***Correspondence Author:** Lipon Chandra Das

*Department of Mathematics, University of Chittagong, Chittagong-4331, Bangladesh
liponbgc@gmail.com, Orcid: <https://orcid.org/0000000181508057>

DOI: - 10.53555/ecb/2024.13.01.38

1. Introduction

Corona viruses constitute a large virus family capable of causing human diseases, now recognized as a global issue. In December 2019, an outbreak of pneumonia cases with an unknown origin emerged in Wuhan.

Today, 504,577,003 cases of covid-19 infection were registered, 6,198,460 deaths Statistics from the Johns Hopkins University website on April 17 22. The initial confirmed case of COVID-19 in Africa was documented in Egypt on February 14, 2020 [1]. By mid-February 2020, China bore a substantial burden of morbidity and mortality, with comparatively lower incidence in other Asian countries, Europe, and North America. Coronaviruses, characterized as enveloped, positive, single-stranded large RNA viruses, infect both humans and a diverse range of animals. Tyrell and Bynno first described coronaviruses in 1966, isolating them from patients with the common cold [2]. Named for their spherical morphology with a core shell and surface projections resembling a solar corona, these viruses are classified into four subfamilies: alpha, beta, gamma, and delta coronaviruses. While alpha and beta coronaviruses typically originate in mammals, particularly bats, gamma and delta viruses have their origins in pigs and birds.

Among the seven subtypes of coronaviruses capable of infecting humans, beta coronaviruses have the potential to cause severe illness and fatalities, while alpha coronaviruses typically lead to asymptomatic or mildly symptomatic infections. SARS-CoV-2, belonging to lineage B of beta coronaviruses, shares close genetic ties with the SARS-CoV virus [3-4]. The primary four structural genes encode the nucleocapsid protein (N), spike protein (S), small membrane protein (SM), and membrane glycoprotein (M), with an additional membrane glycoprotein (HE) present in beta coronaviruses HCoV-OC43 and HKU1 [5]. Symptoms and asymptomatic infections, especially among young children [6]. Observations so far suggest an average incubation period of five days [7] and an average incubation period of 3 days (range: 0-24 days). The proportion of individuals infected with SARS-CoV-2 who remain asymptomatic throughout the course of the infection has not yet been definitively estimated. In symptomatic patients, clinical manifestations usually begin in less than a week, consisting of fever, cough, nasal congestion, fatigue, and other signs of upper respiratory infections. Infection can progress to severe disease with dyspepsia and severe chest symptoms consistent with pneumonia in about

75% of patients, as seen by CT scan at admission [8]. Pneumonia mostly occurs in the second or third week of symptomatic infection. Notable signs of viral pneumonia include reduced oxygen saturation, blood gas abnormalities, changes seen on chest x-rays and other imaging modalities, with ground glass abnormalities, patchy consolidation, alveolar exudates, and interlobular involvement, ultimately indicating worsening. Lymphopenia appears to be widespread and inflammatory markers (C-reactive protein and pro-inflammatory cytokines) are elevated.

In late 2019, an outbreak of a novel human coronavirus, identified as SARS-CoV-2 or COVID-19, originated in Wuhan, China. The virus rapidly spread to 198 countries and territories worldwide, leading to its declaration as a pandemic by the WHO in March 2020 [3]. By March 31, 2020, the global tally included 750,874 confirmed cases of COVID-19, with 36,045 deaths and 117,603 recoveries [9]. Egypt reported the first confirmed case in Africa on February 14, 2020, and by the end of March 2020, the region had surpassed 5,000 confirmed cases [10-11]. Notably, Comoros, Lesotho, Malawi, and South Sudan were the only African countries without a reported confirmed case by March 31, 2020.

Ethiopia, being one of the countries with limited trained human and material resources, is expected to be affected most by the global COVID-19 pandemic. To address this, a strategic approach involves allocating scarce resources for disease prevention and implementing a uniform, evidence-based protocol across all healthcare levels and regions. Centralized command ensures optimal resource utilization. Priority is given to areas most affected, containing the infection locally to prevent widespread impact. Recognizing the necessity for nationwide consistency, the Ethiopian Ministry of Health (FMOH) and Ethiopian Public Health Institute (EPHI) emphasize the development of national COVID-19 prevention and treatment guidelines. A committee, comprising specialists from various fields, is tasked with creating evidence-based, cost-effective guidelines tailored to Ethiopia's culture, living conditions, and background. The aim is to ensure understanding and usability across different levels of healthcare professionals. The prevention and treatment guideline incorporates infection prevention and control principles, covering the entire spectrum from the initial scene to discharge and the safe burial

system in case of death. It delves into the management of critically ill patients, both in regular wards and intensive care units (ICU). Ethical considerations, emphasizing the safety of health professionals and bioethics, are integral to the guideline. Recommendations within this framework are drawn from available studies and guidance from reputable sources like WHO and CDC. Recognizing the evolving nature of the situation, the guideline commits to regular revision and updates based on emerging information and evidence. Healthcare facilities are mandated to ensure thorough training of health professionals, equipping them to implement effective infection control procedures and manage COVID-19 cases [20].

On March 13, 2020, Ethiopia officially confirmed its first case of COVID-19. With a population exceeding 105 million, Ethiopia serves as a migration hub for regional movements within Africa and toward the Gulf. Hosting over 750,000 refugees and marked by trade activities, the country also grapples with one of the world's largest internally displaced populations, primarily stemming from conflicts. The unique mobility environment and regional governance system further complicate the situation. In response to the pandemic, regional governments have implemented individual measures, closing and controlling borders with neighboring regions while restricting internal movements.

The first registered COVID-19 case in Ethiopia, reported on March 15, 2020, was an imported case. As of April 26, 2020, the Ministry of Health reported 305 laboratory-confirmed cases, 5 deaths, and 113 recoveries. These relatively low numbers may be attributed to limited availability of COVID-19 test kits, a lack of community testing beyond airport screening, and undetected individuals with no or mild symptoms not seeking care and thus not being tested. This situation suggests that the reported numbers represent only a fraction of the actual cases, indicating a potentially higher transmission rate, especially from import cases and some cases resulting from personal contacts [19]. In Ethiopia, 85% of the people live isolated in their own low-density areas (farmers, nomads) where media coverage is very poor, almost nil. Thus, research modeling and analysis of data on the spread of infection of diseases is very useful in assessing strategies to control such diseases in populations. Hence, mitigating the profound impact of the disease on people's lives and livelihoods heavily relies on the implementation of effective preventative non-

pharmaceutical interventions (NPIs). NPIs encompass various public health measures designed to reduce viral transmission rates by impacting the reproduction number, representing the average number of secondary cases generated by each case [12-13]. These interventions play a crucial role in shaping the trajectory of the COVID-19 pandemic, influencing its spread and expected duration. However, certain characteristics of the virus, such as the incubation period, serial interval, extent of asymptomatic cases, pre-symptomatic infectiousness, case fatality rate (CFR), and the potential role of weather in transmission, remain ambiguous or poorly understood [14-15].

The majority of reported cases involve asymptomatic or mild presentations, estimated at 80% [16]. The infectious period is also uncertain, with varying estimates ranging from a few days to 10 days or more after the incubation period [17]. The intricate nature of the infection and recovery process underscores the importance of a thorough understanding of the epidemiological dynamics of COVID-19 within the local context to effectively combat the pandemic. Studies illustrating future disease trajectories can aid nations and communities in developing early warning systems, preventing healthcare services overload, minimizing morbidity and mortality, evaluating intervention effects, and assessing the virus's long-term consequences on people's livelihoods.

This necessity is particularly crucial in Africa, where livelihoods are fragile, and past epidemics like HIV/AIDS and more recently, Ebola, have exerted substantial socioeconomic consequences [12-14]. Facing a new pandemic in the region, healthcare systems already strained to deliver essential services such as immunization and HIV/AIDS treatment would be at further risk, potentially jeopardizing the gains achieved in disease control efforts.

1.1 Information Diffusion

The study of information diffusion has a long history within communication research, with abundant intellectual resources. This field encompasses diverse theoretical perspectives, extensive empirical investigations, and numerous analytical models, reflecting the depth and breadth of diffusion research. Specifically, there are a number of lines of diffusion research, such as two-step flow [39, 40], news diffusion [32, 33, 40], diffusion of innovations [44], threshold models [34-37, 45], the Bass diffusion model [28, 29], and

epidemic models [30]. In contemporary times, information diffusion has become a focal point in social media research, drawing scholars from various disciplines. Researchers are dedicated to unraveling the hidden patterns of online information diffusion and understanding the underlying mechanisms. Notably, one crucial diffusion mechanism is the interpersonal effect, rooted in social networks. Network epidemic models, particularly on complex networks like scale-free networks, indicate that information has the potential to infect a substantial proportion of the population. The study of these models reveals that, especially in networks with a long-tailed degree distribution, the threshold of generic epidemic models is either vanishing or finite. Consequently, there is a tendency for a global cascade of information diffusion on the Internet [43]. Global cascades signify significant diffusion, suggesting that more than a fixed fraction of the large but finite networks has been activated to spread the information.

1.2 News Diffusion

Another line of research on information diffusion focuses on one specific category of information news. News diffusion is the process of news flowing from news sources to audiences. Beginning in the 1940s, increasing during the 1960s-1980s, and decreasing in the 1990s, classic studies of news diffusion compared media effect and interpersonal effects by studying the diffusion channels, cumulative diffusion curves, and the determinants of news diffusion [41]. Miller's pioneering study in 1945 marked the inception of news diffusion research, establishing a tradition of assessing the impacts of various diffusion

channels [42]. Focused on the diffusion of news regarding Roosevelt's death among 143 students at Kent State University, Miller found that 85% of the students learned the news through word of mouth. News diffusion, as a common body of knowledge, integrates into community life, reaching people through both mass media and interpersonal channels. It is a social process involving cumulative growth in the number of individuals informed about news events at both aggregate and individual levels.

In the diffusion process, social actors interact with the social structure, shaping news diffusion through agency and structure. From an agency perspective, news diffusion is conceptualized as the flow of public attention, driven by individuals' needs and motivations. Treating news as a form of knowledge and diffusion as a learning process, individuals' exposure to news leads to awareness generated through news-learning. Two critical factors influencing the size of news diffusion are the limited capacity of individuals' attention [38] and selective attention [45, 46].

Social structure also plays a role in shaping the diffusion process. The J-curve model of news diffusion posits a curvilinear relationship between the percentage of news awareness and the percentage of interpersonal sources [31-33]. Previous studies on 18 news events, examining the size of diffusion and media differences, identified a J-curve relationship: breaking news is primarily learned from interpersonal sources, while less crucial news is obtained from mass media (Figure 3).

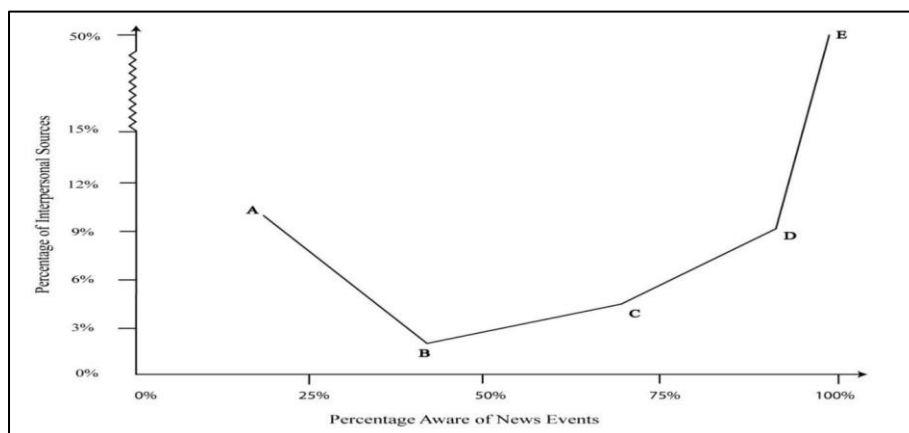


Figure 1: Diffusion through Personal Source⁸ by Awareness of News Event (source, Greenberg (1964b)).

There are numerous pressing questions surrounding the spread of COVID-19, including inquiries about future infection rates, the timing of the infection rate's inflection point, the number

of infections during the peak period, and the effectiveness of existing interventions. With COVID-19 being a novel coronavirus discovered in December 2019, data on the outbreak remains

insufficient, and available information is still in the early stages of exploration through means such as clinical trials [18].

In this study, an SEIR model is formulated and analyzed to examine the impact of media influence, facilitated by information dissemination, on the spread of the COVID-19 pandemic in a variable population with immigration. The modeling process assumes that the growth rate of cumulative awareness programs, driven by the media, is dependent on the number of infected individuals present in the population. Additionally, awareness about the disease prompts susceptible individuals to isolate themselves, forming a distinct class to avoid infection. The model also accounts for the depletion of awareness programs over time. Conceptually, the proposed model envisions the coexistence of two strains contributing to the COVID-19 pandemic disease [27-28].

2. The Model Formulation

Following the onset of the COVID-19 pandemic, the Chinese government implemented various impactful measures to address the outbreak. These measures included inspection detention, isolation treatment, quarantine of cities, and the suspension of traffic on major roads [21, 22, 26].

However, the traditional SEIR model falls short in capturing the nuanced effects of these interventions on different populations. Based on the analysis of the actual situation and available data, we divided the population into different warehouses and created a more efficient model for the dynamic spread of infectious diseases.

Considering the current epidemic situation, we have classified the population in Ethiopia into seven distinct categories, as outlined in Table 1. Given the incubation period of COVID-19 ranging from 2 to 14 days, there are already infected but not diagnosed individuals (E) in the natural environment of the susceptible population (S) when the first case is detected. Some people who have been infected must go through a certain incubation period before suspected symptoms can be detected (S_q). Chest CT was used to see if there were glass shadows in the lungs to determine if the diagnosis was conformed (I_D), ignorant infected individuals with severe symptoms (I_s), awareness disappears Virus-infected and highly awarded infectious (I_a) and after a period of quarantine treatment these two groups of people will recover from the hospital (R), or face death due to underlying illnesses.

Table 1 Variables for the basic COVID-19 model

Variables	Description
$S(t)$	Individuals who are susceptible to being infected by the virus at a given time t
$E(t)$	Infected with the virus but without the typical symptoms of infection at time t
$I_a(t)$	Infected with the virus and highly awarded infectious at time t
$I_s(t)$	Infected individuals with severe symptoms at time t
$I_D(t)$	Infected individuals Diagnosed and quarantined at time t
$S_q(t)$	Number of People self-quarantine susceptible at time t
$R(t)$	Number of people who are cured after infection at time t
$N(t)$	Total human population at time t

Table 2 Parameters and their interpretations for the COVID-19 model

Parameter	Description
β	The incidence rate of susceptible population
q	Transfer rate of humans from susceptible to self-quarantine susceptible
q_1	Transfer rate of self-quarantine susceptible to susceptible after medical diagnosis
μ	Transfer rate of confirmed laboratory positive case
ω	Transfer rate of awarded cure or died to recovered
ϵ	Transfer rate of medical diagnosis cure or died to recovered
Ψ	The recruitment rate at which new individuals enter in the Ethiopian population
$(1 - \gamma)\psi$	Reduction of exposed to severe infected
λ	Natural death rate
$\gamma\psi$	Transfer of rate at the proportion of latent persons who were converted to free infection awarded humans

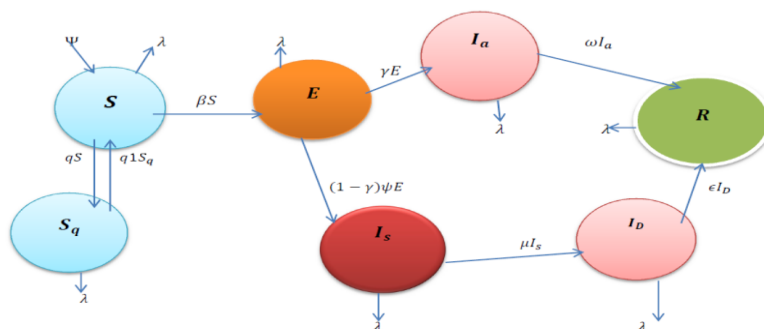


Figure 2: depicts the COVID-19 transmission model, highlighting the spread of disease awareness information via news media.

The diagram illustrates the epidemiological transitions in the baseline transmission model through black arrows. Susceptible individuals (S) transition to latent infection (E) through the force of infection resulting from contact with infectious individuals in two distinct classes (I_a and I_s). Individuals leave the E compartment at rate $\gamma\psi$. A proportion γ of the latently infected individuals (E) will go to the I_a compartment, and the proportion $(1 - \gamma)$ of E individuals will go to the I_s compartment. Infectious individuals with mild symptoms (I_a) recovered at rate ω . Individuals with severe symptoms (I_s) are diagnosed and kept in isolation (I_D) at rate ϵ they recover (R) or die. Table 1 and 2 provides the description and values of all parameters.

Utilizing the assumptions, definitions of individual variables, and parameters outlined in Tables 1 and 2, this section formulates and presents a system of nonlinear differential equations that describe the dynamic transmission of the COVID-19 pandemic disease facilitated by media communication.

$$\frac{dS}{dt} = \Psi - \frac{\beta S I_a}{N} - (\lambda + q)S + q1S_q$$

$$\frac{dE}{dt} = \frac{\beta S I_a}{N} - (\gamma + \lambda + \psi - \gamma\psi)E \tag{1}$$

$$\frac{dI_a}{dt} = \gamma\psi E - (\lambda + \omega)I_a$$

$$\frac{dI_s}{dt} = (1 - \gamma)\psi E + (\lambda + \mu)I_s$$

$$\frac{dI_D}{dt} = \mu I_s - (\lambda + \epsilon)I_D$$

$$\frac{dR}{dt} = \omega I_a + \epsilon I_D - \lambda R$$

$$\frac{dS_q}{dt} = qS - (\lambda + q1)S_q$$

with initial conditions: -

$S(0) > S_0, E(0) \geq E_0, S_q(0) > S_{q0}, I_a(0) \geq I_{a0}, I_s(0) \geq I_{s0}, I_D(0) \geq I_{D0}, R(0) > R_0$. The total number of population size is $N = S + E + S_q + I_a + I_s + I_D + R$ with their differential.

3. Media awareness and information diffusion analysis of the COVID-19 Pandemic

3.1 Non-Negativity of Solution

We analyze the model to check if media awareness has any effect on diseases, i.e. whether the disease will be eradicated or not. Threshold parameters, crucial for determining the persistence or elimination of COVID-19, will be identified and examined. Therefore, we start by defining an invariant region to test whether the model is biologically meaningful and to show that all solutions 0 of (1) are positive for all $t \geq 0$ and are attracted in that region.

Theorem 3.1. Each solution of the $SES_qI_aI_sI_DR$ model structure (1) with preliminary stipulations subsists in the interval $[0, \infty)$ and $S(t) > 0, S_q(t) \geq 0, E(t) \geq 0, I_a(t) \geq 0, I_s(t) \geq 0, I_D(t) \geq 0$ as well as $R(t) > 0$ for all values of $t \geq 0$.

Proof. As the right hand side of $SES_qI_aI_sI_DR$ model structure (1) is completely continuous and locally Lip-Schitzian on C , the solution $(S(t), S_q(t), E(t), I_a(t), I_s(t), I_D(t), R(t))$ with initial conditions exists, and is unique on $[0, \zeta)$, where 0

$< \zeta < \infty$. From system (1) with initial condition, we have

$$\frac{ds}{dt} > -AS(t), S(t) \geq S(0) \exp[-At] > 0 \quad (2)$$

The second equation of the system implies

$$\frac{dE}{dt} \geq -BE(t), E(t) \geq E(0) \exp[-Bt] \geq 0 \quad (3)$$

Again from the system (1) we have

$$\frac{dS_q}{dt} > -CS_q(t), S_q(t) \geq S_q(0) \exp[-Ct] > 0 \quad (4)$$

$$\frac{dI_a}{dt} \geq -DI_a(t), I_a(t) \geq I_a(0) \exp[-Dt] \geq 0 \quad (5)$$

$$\frac{dI_s}{dt} \geq -DI_s(t), I_s(t) \geq I_s(0) \exp[-Et] \geq 0 \quad (6)$$

$$\frac{dI_D}{dt} \geq -DI_D(t), I_D(t) \geq I_D(0) \exp[-Ft] \geq 0 \quad (7)$$

$$\frac{dR}{dt} > -GR(t), R(t) \geq R(0) \exp[-Gt] > 0 \quad (8)$$

3.2 Invariant Region

The total population sizes are $N = S + S_q + E + I_a + I_s + I_D + R$ with their differential equations.

$$\frac{dN}{dt} = \frac{dS}{dt} + \frac{dS_q}{dt} + \frac{dE}{dt} + \frac{dI_a}{dt} + \frac{dI_s}{dt} + \frac{dI_D}{dt} + \frac{dR}{dt} = \Psi - \lambda N \quad (9)$$

Theorem 3.2. *The solutions of the system (1) are feasible for all $t \geq 0$ if they enter the invariant region Ω .*

Proof. Let $(S, S_q, E, I_a, I_s, I_D, R) \in \mathbb{R}^{7+}$ be any solution of the system (1) with non-negative initial conditions.

$$\frac{dN}{dt} \leq \Psi - \lambda N, \frac{dN}{dt} + \lambda N \leq \Psi \quad (10)$$

The integrating factor for (10) is

$$(IF) = e^{\int -\lambda dt} = e^{-\lambda t}$$

Multiplying both side of (10) by $e^{-\lambda t}$ gives

$$e^{-\lambda t} \frac{dN}{dt} + \lambda N e^{-\lambda t} \leq \Psi e^{-\lambda t} \quad (11)$$

ntegrating on both sides of (10) we have

$$\lambda N e^{-\lambda t} \leq \frac{\Psi}{\lambda} e^{-\lambda t} + c$$

Where c is a constant of integration.

Dividing through (11) by $e^{-\lambda t}$ + gives

$$\lambda N e^{-\lambda t} \leq \frac{\Psi}{\lambda} e^{-\lambda t} + c \quad (12)$$

Using the initial conditions at $t = 0, N_0 = 0$

$$N_0 \leq \frac{\Psi}{\lambda} + c \Rightarrow N_0 - \frac{\Psi}{\lambda} \leq c \quad (13)$$

Substitute in equation (13) we can get

$$N \leq \frac{\Psi}{\lambda} + \left(N_0 - \frac{\Psi}{\lambda}\right) e^{-\lambda t} \quad (14)$$

Applying the theorem of differential inequality [23], we obtain.

$$0 \leq N \leq \frac{\Psi}{\lambda} \text{ as } t \rightarrow \infty$$

Therefore, as $t \rightarrow \infty$ in (14), the human population N , approaches $k = \frac{\Psi}{\lambda}$ (that is $N \rightarrow k = \frac{\Psi}{\lambda}$), the parameters $k = \frac{\Psi}{\lambda}$ is usually called the carrying capacity [27].

Hence all feasible solutions set of the human population of the model (1) enters the region.

$$\Omega = \left((S, S_q, E, I_a, I_s, I_D, R) \in \mathbb{R}^{7+} : S > 0, S_q \geq 0, E \geq 0, I_a \geq 0, I_s \geq 0, I_D \geq 0, R > 0, N \leq \frac{\Psi}{\lambda} \right)$$

Therefore, the region Ω is positively invariant (i.e. solutions remain positive for all times, t) and in the model (1) is biologically meaningful and mathematically well-posed in the domain Ω .

3.3 Existence of Equilibrium points without disease E_0

Steady state solutions or equilibrium points are the roots or solutions of the system of equations when the right-hand side of a nonlinear system is set to zero. That is, using the nonlinear system (1) we have

$$\begin{aligned} \Psi - \frac{\beta S I_a}{N} - (\lambda + q)S + q1S_q &= 0 \\ \frac{\beta S I_a}{N} + (\gamma + \lambda + \psi - \gamma\psi)E &= 0 \quad (15) \\ \gamma\psi E - (\lambda + \omega)I_a &= 0 \end{aligned}$$

$$\begin{aligned} (1 - \gamma)\psi E + (\lambda + \mu)I_s &= 0 \\ \mu I_s - (\lambda + \epsilon)I_D &= 0 \end{aligned}$$

$$\begin{aligned} \omega I_a + \epsilon I_D - \lambda R &= 0 \\ qS - (\lambda + q1)S_q &= 0 \end{aligned}$$

Let $(S^*, S_q^*, E^*, I_a^*, I_s^*, I_D^*, R^*)$ be the steady state of (1) which can obtain by solving (15). Disease free equilibrium points (DFE) are steady

state solutions where there is no COVID 19 conformed in the population that is S, S_q, E, I_a, I_s, I_D and R .

In absence of the disease, this implies that $E = I_a = I_s = I_D = R = 0$ therefore (15) reduces to

$$\left. \begin{aligned} \Psi - (\lambda + q)S &= 0 \\ qS - (\lambda + q1)S_q &= 0 \end{aligned} \right\} \quad (16)$$

This implies that

$$\left. \begin{aligned} S^* &= \frac{\Psi}{\lambda + q} \\ S_q^* &= \frac{q\Psi}{(\lambda + q)(\lambda + q1)} \end{aligned} \right\} \quad (17)$$

Therefore, the equilibrium point of the COVID-19 model (1) is given by,

$$E_0 = (S^*, S_q^*, E^*, I_a^*, I_s^*, I_D^*, R^*) = \left(\frac{\Psi}{\lambda + q}, \frac{q\Psi}{(\lambda + q)(\lambda + q1)}, 0, 0, 0, 0, 0 \right) \quad (18)$$

This signifies the state in which there is no infection, indicating the absence of COVID-19 cases within the society.

4. Basic Reproduction Number (R_0)

Reproduction number, denoted by R_0 , is the threshold or a level for many epidemiological models. It determines whether a disease can attack the population or not. The threshold quantity R_0 indicates the number of new infected individuals is produced by one infected individual. When $R_0 < 1$ each infected individual propagates the infection and produces on average less than one new infected individual so that the disease is expected to die out completely over time. On the other hand, if $R_0 > 1$, each individual produces more than one new infected individual so we would expect the disease to spread more and grow in the population. This means that the value of threshold quantity R_0 in order to eradicate the disease must be reduced by less than one.

The following steps are followed to compute the basic reproduction number R_0 . The basic reproduction number cannot be determined from the structure of the mathematical model alone, but depends on the definition of infected and uninfected compartments. Assuming that there are n compartments of which the first m

compartments to infected individuals. That is the parameters may be vary compartment to compartment, but are the identical for all individuals within a given compartment. Let

$$X_i = (x_1, x_2, \dots, x_n), \quad X_i \geq 0 \text{ for all, } i = 1, 2, \dots, m$$

Be the vector of human and mosquito individuals in each compartment. Let us sort the compartments so that first m compartments infected individuals.

Let $F_i(x)$ be the rate of appearance of new infections in compartment i .

$$V_i(x) = V^-_i(x) - V^+_i(x) \text{ Where } V^+_i(x) \text{ is}$$

rate of transfer of individuals into compartment i by all other means and $V^-_i(x)$ is the rate of transfer of individual out of the i^{th} compartment.

It is assumed that each function is continuously differentiable at least twice in each variable. The disease transmission model consists of non-negative initial conditions together with the following system of equations:

$$\frac{dx_i}{dt} = f_i(x) = F_i(x) - V_i(x), \quad i = 1, 2, 3, \dots, n$$

Where $\frac{dx_i}{dt}$ is the rate of change of x . The next is the computation of the square matrices F and V of order $(m \times m)$, where m is the number of infected classes, defined by $F = \left[\frac{dF_i(x)}{dx_j} (x_0) \right]$ and $V = \left[\frac{dV_i(x)}{dx_i} (x_0) \right]$ with $1 \leq i, j \leq m$, such that F is non-negative, V is non-singular matrix and x_0 is the disease-free equilibrium point (DFE). Since F is non-negative and V is non-singular, then V^{-1} is non-negative and also FV^{-1} is non-negative. Hence the FV^{-1} is called the next generation matrix for the model. Finally, the basic reproduction number R_0 is given by

$$R_0 = \gamma(FV^{-1})$$

Where $\gamma(A)$ denotes the spectral radius of matrix A and the spectral radius is the biggest non-negative eigenvalue of the next generation matrix. Rewriting model system (1) starting with the infected compartments for the population; $S, S_q, E, I_a, I_s, I_D, R$ and then following by uninfected classes; S, S_q, R , also from the population, then the model system becomes

$$\left. \begin{aligned} \frac{dE}{dt} &= \frac{\beta SI_a}{N} + (\gamma + \lambda + \psi - \gamma\psi)E \\ \frac{dI_a}{dt} &= \gamma\psi E - (\lambda + \omega)I_a \\ \frac{dI_s}{dt} &= (1 - \gamma)\psi E + (\lambda + \mu)I_s \\ \frac{dI_D}{dt} &= \mu I_s - (\lambda + \epsilon)I_D \\ \frac{dS}{dt} &= \Psi - \frac{\beta SI_a}{N} - (\lambda + q)S + q1S_q \\ \frac{dS_q}{dt} &= qS - (\lambda + q1)S_q \\ \frac{dR}{dt} &= \omega I_a + \epsilon I_D - \lambda R \end{aligned} \right\} \quad (19)$$

$$F(x) = \begin{bmatrix} \frac{\beta SI_a}{N} \\ 0 \\ 0 \\ 0 \end{bmatrix} \quad V(x) = \begin{bmatrix} (\gamma + \lambda + \psi - \gamma\psi)E \\ \gamma\psi E - (\lambda + \omega)I_a \\ (1 - \gamma)\psi E + (\lambda + \mu)I_s \\ \mu I_s - (\lambda + \epsilon)I_D \end{bmatrix}$$

The partial derivatives of (19) with respect to (I_a) and the jacobian matrix of F_i at the disease-free equilibrium point (18) is:-

$$F = \begin{bmatrix} 0 & \beta & 0 & 0 \\ 0 & 0 & 0 & 0 \\ 0 & 0 & 0 & 0 \\ 0 & 0 & 0 & 0 \end{bmatrix}$$

Similarly, the partial derivatives of (19) with respect to (E, I_a, I_s, I_D) and the jacobian matrix v is:-

From the system of equations (19) F_i and V_i are defined as

$$v = \begin{bmatrix} (\gamma + \lambda + \psi - \gamma\psi) & 0 & 0 & 0 \\ 0 & -(\lambda + \omega) & 0 & 0 \\ (1 - \gamma)\psi & 0 & (\lambda + \mu) & 0 \\ 0 & 0 & \mu & -(\lambda + \epsilon) \end{bmatrix}$$

$$v^{-1} = \begin{bmatrix} \frac{1}{(\gamma + \lambda + \psi - \gamma\psi)} & 0 & 0 & 0 \\ 0 & \frac{1}{(\lambda + \omega)} & 0 & 0 \\ \frac{1}{(1 - \gamma)\psi} & 0 & \frac{1}{\lambda + \mu} & 0 \\ 0 & 0 & \frac{\mu}{\lambda + \epsilon} & \frac{1}{\lambda + \epsilon} \end{bmatrix}$$

From Fv^{-1} , we can determine the eigenvalues of the basic reproduction number R_0 by taking the spectral radius (dominant eigenvalue) of the matrix Fv^{-1} . Thus it is calculated as $|A - \lambda A| = 0$. We determine the expression for R_0 using the next generation matrix approach [18] as $R_0 = \frac{\gamma\beta}{(\gamma + (1 - \gamma)\psi + \lambda)}$. Further, it can be verified that the disease free equilibrium point E_0 given by (18) is locally asymptotically stable if $R_0 < 1$ and unstable if $R_0 > 1$.

5. Numerical simulation and Discussion

In this section, we delve into the numerical simulation and discussion of the system of differential equations provided in (1). As mentioned earlier, these equations encapsulate the dynamics of human populations within the COVID-19 model, accounting for the influence of awareness programs. The simulation study employed the ode45 solver within the MATLAB software, utilizing the fourth-

order Runge-Kutta method with a variable step size. Parametric values were sourced from the literature and applied accordingly, specifically drawing from research conducted in malaria-endemic countries sharing similar environmental conditions with our nation. The chosen values align with the current COVID-19 pandemics were consistent with cases and mortality rates. A numerical analysis of model (1) is presented.

$S(0) = 1000,000, E(0) = 33,385,$
 $S_q(0) = 319,000, I_a(0) = 1,311, I_s(0) = 65,$
 $I_D(0) = 54,980, R(0) = 7,911.$ Furthermore, to validate the feasibility of our analysis concerning stability conditions, we conducted numerical computations using MATLAB 7.5.0. We selected a specific set of parameter values in the model system (1) for this purpose.

$$\begin{aligned} \Psi &= 500, \beta = 0.0004, q = 0.0007, q_1 \\ &= 0.0003, \epsilon = 0.3, \\ \lambda &= 0.006, \omega = 0.002, \gamma = 0.001, \psi = 0.2, \mu_1 \\ &= 0.0023 \end{aligned}$$

We formulated a fundamental COVID-19 model to elucidate the impact of varying intervention parameters [20] and [25–26]. Figure 2 presents a phase portrait illustrating changes in seven state variables. The model estimates the dynamics of COVID-19 over time, considering susceptible individuals, those in self-quarantine, exposed individuals, infectious awarded individuals, non-infected individuals in isolation, infected and diagnosed individuals, and individuals who have recovered or been removed from the system.

The variation of infective population $I_S(t)$ and $I_D(t)$ and awareness programs $I_a(t)$ with respect to time 't' for different values of the

transmission rate of ' γ ' and ' ω ' shown in Figures 4, 5 and 6 respectively. From these figures, it noted that as the transmission rate of ' γ ' increases the number of recovered humans $R(t)$ and awareness programs and information diffusion through media both decreases the infected humans sever infected and infected diagnosed humans increased in number. Further, the variations of the infective population $I_S(t)$ and the aware population $I_a(t)$ with respect to time 't' for different values of rate of transmission of awareness programs or the awarded cure or died ' ω ' were show in Figures. 5 and 6 respectively. From these figures, it is apparent that as the rate of transmission of awareness programs ' ω ' increases the infective population $I_S(t)$ decreases whereas the aware population $I_a(t)$ increases. In addition, from Figure 6 it is interesting to observe that for $\gamma = 0$ the aware population $I_S(t)$ and $I_D(t)$ approaches 0.

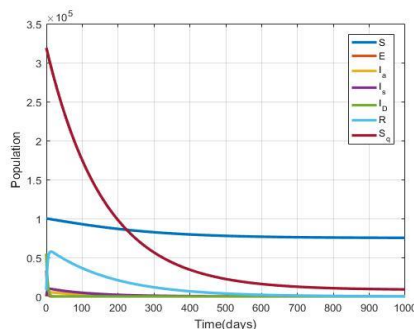


Figure 3 portrays the dynamic changes in seven state variables within the COVID-19 model

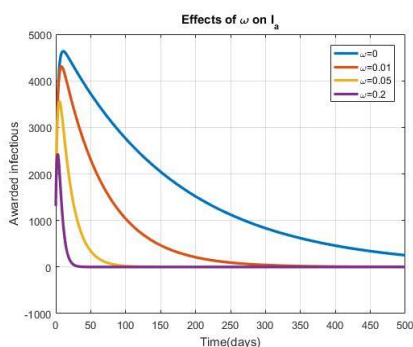


Figure 4. Variation of awarded infective population with time for different values of ω .

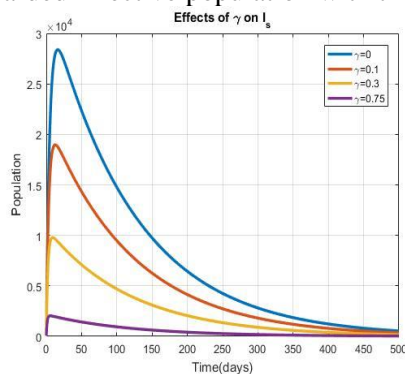


Figure 5. Variation of severe infective population with time for different values of γ .

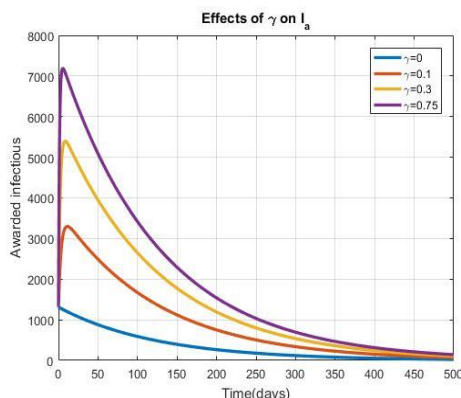


Figure 6. Variation of awarded infective population with time for different values of γ .

6. Conclusion

We have developed and examined a fundamental deterministic mathematical model to enhance our understanding of controlling the spread of the COVID-19 pandemic. The proposed model considers the impact of media-driven awareness programs on a population variable, incorporating immigration and information diffusion through media. Through theoretical analysis, we describe the dynamic process of coupled information diffusion, particularly in the context of social media transmission.

The model suggests that the growth rate of the cumulative density of awareness programs is proportionally linked to the number of infected, isolated infected, and infected individuals. Additionally, awareness is seen to prompt some individuals to isolate or self-isolate, forming a distinct subclass within the population. The model indicates that the disease-free equilibrium remains stable until the basic reproduction number becomes unstable. This instability leads to the existence of an endemic equilibrium, which is shown to be both locally and non-linearly stable under certain conditions.

Several implications arise from our findings: (1) Implementing internet regulation may impact information diffusion clarity, but it could also decrease transparency. Therefore, prompt government disclosure of epidemic information through press conferences is crucial for transparent information diffusion. Official media can serve as a guide, consistently updating the public on the epidemic. (2) Supervision of information diffusion needs strengthening to counteract the spread of false or alarmist information on social media. Authorities, institutions, and experts should swiftly refute misinformation to prevent adverse social or media influences. (3) Recognizing the urban-

rural internet penetration gap in Ethiopia, timely official documents should be issued at all government levels to transmit information to rural areas. Finally, model analysis also shows that awareness programs through media influence and information diffusion are useful in reducing the spread of COVID-19 pandemic diseases by isolating those susceptible from infectious diseases

References

1. Coronavirus 2019-nCoV, CSSE. Coronavirus 2019-nCoV Global Cases by Johns Hopkins CSSE (Available from: <https://gisanddata.maps.arcgis.com/apps/opsdashboard/index>).
2. Tyrrell DA, Bynoe ML. Cultivation of viruses from a high proportion of patients with colds. *Lancet* 1966; 1: 76–77.
3. GISAID Global Initiative on Sharing All Influenza Data Phylogeny of SARS-like beta coronaviruses including novel coronavirus (nCoV). (Available from: <https://nextstrain>).
4. Zhou P, Yang XL, Wang XG et al. A pneumonia outbreak associated with a new coronavirus of probable bat origin. *Nature* 2020. <https://doi.org/10.1038/s41586-020-2012-7>
5. Rottier PJM. The Coronaviridae Siddell SG, editor. 115-137-2013. Springer Science & Business Media. (Available from: https://link.springer.com/content/pdf/10.1007%2F978-1-4899%20153-3_6.pdf).
6. Chan JF, Yuan S, Kok KH et al. A familial cluster of pneumonia associated with the 2019 novel coronavirus indicating person-to-person transmission: a study of a family cluster *Lancet* 2020. S0140-6736(20)30154-9. [https://doi.org/10.1016/S0140-6736\(20\)30154-9](https://doi.org/10.1016/S0140-6736(20)30154-9)

7. Li Q, Guan X, Wu P et al. Early transmission dynamics in Wuhan, China, of novel coronavirus-infected pneumonia. *N Engl J Med* 2020. <https://doi.org/10.1056/NEJMoa2001316>
8. Guan W, Ni Z, Yu H, et al. Clinical characteristics of 2019 novel coronavirus infection in China, medRxiv preprint posted online on Feb. 9, 2020; <https://doi.org/10.1101/2020.02.06.20020974>.
9. WHO COVID-19 data accessed April 3 2020
10. African CDC <https://africacdc.org/covid-19/> accessed April 2 2020
11. WHO EMRO <http://www.emro.who.int/index.html> accessed April 6 2020
12. Ferguson N.M, Laydon. D, Nedjati-Gilani. G, Imai.N, Ainslie.K, Baguelin.M, Bhatia.S, Boonyasiri A. Impact of non-pharmaceutical interventions (NPIs) to reduce COVID-19 mortality and healthcare demand. London: Imperial College COVID-19 Response Team, March 16 (2020). Imperial College accessed March 23 2020
13. Murray. C. JL, IHME COVID-19 health service utilization forecasting team. Forecasting COVID-19 impact on hospital bed-days, ICU-days, ventilator-days and deaths by US state in the next 4 months 2020.03.27.20043752; <https://doi.org/10.1101/2020.03.27.20043752>
14. WHO Coronavirus disease (COVID2019) situation report-30 https://www.who.int/docs/defaultsource/coronaviruses/situation-reports/20200219-sitrep-30-covid19.pdf?sfvrsn=3346b04f_2 accessed March 31 2020
15. Martinez-Alvarez.M, Jarde.A, Usuf.E, Brotherton.H, Bittaye.M, Samateh Al, Antonio. M et.al., COVID-19 pandemic in West Africa *Lancet Glob Health* April 1, 2020
16. Zou L Ruan F, Huang M, Liang L, Huang H, Hong Z, Yu J, et.al., SARS-CoV2 viral load in upper respiratory specimens of infected patients. *N Engl J Med* 2020; 382:1177-1179
17. Kinfu. Y, Opiyo.C, & Wamukoya, M. (2014). Child Health and Mortality in sub-Saharan Africa: Trends, causes, and forecasts. In C. O. Odimegwu, & J. Kekovole (Eds.), *Continuity and change in sub-saharan African Demography* (Vol. 17, pp. 60-77) (Routledge African Studies; Vol. 17). New York, USA: Routledge
<https://doi.org/10.4324/9781315879444>
18. Ma ZE, Zhou YC, Wang WD. *Mathematical modeling and research of infectious disease dynamics*. 2004.
19. IOM east and horn of Africa regional strategic preparedness and response plan covid-19, updated on 6 April 2020, 2020.04.09.20059154v1
20. FMOH national comprehensive covid-19 management handbook Ethiopia First edition APRIL 2020
21. Li Y, Wang B, Peng R, Zhou C, Zhan Y, Liu Z, et al. *Mathematical Modeling and Epidemic Prediction of COVID-19 and Its Significance to Epidemic Prevention and Control Measures* *Ann Infect Dis Epidemiology*. 2020; 5(1): 1052. ISSN: 2475-5664
22. Stephen E. Moore. and Eric Okyere *Controlling the Transmission Dynamics of COVID-19* arXiv:2004.00443V2, 2 April ,2020
23. Birkhoff, G and Rota, G.C (1982), *Ordinary Differential Equations*, Ginn.
24. Fekadu Tadege Kobe "*SEIR Model and Simulation for Controlling Malaria Diseases Transmission without Intervention Strategies*" Published in *International Journal of Trend in Scientific Research and Development* (ijtsrd), ISSN: 2456 6470, Volume -3 Issue-6, Oct 2019, pp.151 <https://www.ijtsrd.com/papers/ijtsrd25235.pdf>
25. K. Misraa,*, Anupama Sharmaa, J.B. Shuklab,c, *Modeling and analysis of effects of awareness programs by media on the spread of infectious diseases* *Mathematical and Computer Modelling* 53 (2011) 1221–1228 doi:10.1016/j.mcm.2010.12.005.
26. Fekadu Tadege Kobe, Purnachandra Rao Koya. *Modeling and Analysis of Effect of Awareness Programs by Media on the Spread of COVID19 Pandemic Disease*. *American Journal of Applied Mathematics*. Vol. 8, No. 4, 2020, pp. 223-229. doi: 10.11648/j.ajam.20200804.17.
27. Namawejje H. (2011). *Modelling the Effect of Stress on the Dynamics and Treatment of Tuberculosis*. M.Sc. (Mathematical Modelling) Dissertation, University of Dares Salaam, Tanzania
28. Bass, F. (1969). *A New Product Growth Model for Consumer Durables*. *Management science*, 15(5), 215-227.

29. Bass, F. (2004). Comments on "A new product growth for model consumer durables": The Bass Model. *Management science*, 50(12), 1833-1840.

30. Becker, N. G. (1992). Infectious diseases of humans: Dynamics and control. *Australian Journal of Public Health*, 16(2), 208-209.

31. DeFleur, M. L. (1987). The growth and decline of research on the diffusion of the news, 1945- 1985. *Communication Research*, 14(1), 109-130.

32. Greenberg, B. S. (1964a). Diffusion of news of the Kennedy assassination. *Public Opinion Quarterly*, 28(2), 225-232.

33. Greenberg, B. S. (1964b). Person to person communication in the diffusion of a news event. *Journalism Quarterly*, 41(3), 489-494.

34. Granovetter, M. (1978). Threshold models of collective behavior. *American Journal of Sociology*, 83(6), 1420-1443.

35. Granovetter, M., & Soong, R. (1983). Threshold models of diffusion and collective behavior. *The Journal of Mathematical Sociology*, 9(3), 165-179.

36. Granovetter, M., & Soong, R. (1986). Threshold models of interpersonal effects in consumer demand. *Journal of Economic Behavior and Organization*, 7(1), 83-99.

37. Granovetter, M., & Soong, R. (1988). Threshold models of diversity: Chinese restaurants, residential segregation, and the spiral of silence. *Sociological Methodology*, 18(6), 69- 104.

38. Kahneman, D. (1973). *Attention and effort*. Englewood Cliffs, NJ: Prentice-Hall.

39. Katz, E. (1957). The two-step flow of communication: An up-to-date report on an hypothesis. *Public Opinion Quarterly*, 21(1), 61-78. doi: 10.1086/266687

40. Katz, E., & Lazarsfeld, P. F. (1955). *Personal influence: The part played by people in the flow of mass communications*. New York: Free Press.

41. Larsen, O. N., & Hill, R. J. (1954). Mass media and interpersonal communication in the diffusion of a news event. *American Sociological Review*, 19(4), 426-433.

42. Miller, D. C. (1945). A research note on mass communication: How our community heard about the death of president Roosevelt. *American Sociological Review*, 10(5), 691-694.

43. Pastor-Satorras, R., & Vespignani, A. (2001). Epidemic spreading in scale-free networks. *Physical review letters*, 86(14), 3200-3203.

44. Rogers, E. M. (1983). *Diffusion of innovations* (3rd ed.). New York: The free press.

45. Treisman, A., & Fearnley, S. (1969). The Stroop test: Selective attention to colours and words. *Nature*, 222, 437-439.

46. Treisman, A. M. (1964). Selective attention in man. *British Medical Bulletin*, 20(1), 12-16.

47. Valente, T. W. (1995). *Network models of the diffusion of innovations*. Cresskill, New Jersey: Hampton press.

48. S. Ghosh and L. C. Das, "Using Data Mining Techniques for COVID-19: A Systematic Review," *Int. J. Data Sci. Technol.*, vol. 8, no. 2, pp. 36-42, 2022.

Appendix: MATLAB

function dejen=corona_fekaduooverlab1(t,x)
 global Psi beta lamda q q1 gamma psi omega mu
 epsilon N...

gamma1 omega1 gamma2 omega2 gamma3
 omega3

N=x(1)+x(2)+x(3)+x(4)+x(5)+x(6)+x(7);
 dejen=[Psi- beta*x(1)*x(3)/N-
 (lamda+q)*x(1)+q1*x(7);

beta*x(1)*x(3)/N-(gamma+lamda+psi-
 gamma*psi)*x(2);

gamma*psi*x(2)-(lamda+omega)*x(3);
 (1-gamma)*psi*x(2)-(lamda+mu)*x(4);
 mu*x(4)-(lamda+epsilon)*x(5);
 omega*x(3)+epsilon*x(5)-lamda*x(6);
 q*x(1)-(lamda+q1)*x(7);
 Psi- beta*x(8)*x(10)/N-

(lamda+q)*x(8)+q1*x(14);
 beta*x(8)*x(10)/N-(gamma1+lamda+psi-
 gamma1*psi)*x(9);

gamma1*psi*x(9)-(lamda+omega1)*x(10);
 (1-gamma1)*psi*x(9)-(lamda+mu)*x(11);
 mu*x(11)-(lamda+epsilon)*x(12);
 omega1*x(10)+epsilon*x(12)-lamda*x(13);
 q*x(8)-(lamda+q1)*x(14);
 Psi- beta*x(15)*x(17)/N-

(lamda+q)*x(15)+q1*x(21);
 beta*x(15)*x(17)/N-(gamma2+lamda+psi-
 gamma2*psi)*x(16);

gamma2*psi*x(16)-(lamda+omega2)*x(17);
 (1-gamma2)*psi*x(16)-(lamda+mu)*x(18);
 mu*x(18)-(lamda+epsilon)*x(19);
 omega2*x(17)+epsilon*x(19)-lamda*x(20);
 q*x(15)-(lamda+q1)*x(21);
 Psi- beta*x(22)*x(24)/N-

(lamda+q)*x(22)+q1*x(28);
 beta*x(22)*x(24)/N-(gamma3+lamda+psi-
 gamma3*psi)*x(23);

gamma3*psi*x(23)-(lamda+omega3)*x(24);
 (1-gamma3)*psi*x(23)-(lamda+mu)*x(25);

```
mu*x(25)-(lamda+epsilon)*x(26);          grid on
omega3*x(24)+epsilon*x(26)-lamda*x(27);
q*x(22)-(lamda+q1)*x(28);];
```

```
global Psi beta lamda q q1 gamma psi omega mu
epsilon ...
gamma1 omega1 gamma2 omega2 gamma3
omega3
```

```
Psi=500; beta=0.0004; lamda=0.006; q=0.0007;
q1=0.0003;
gamma=0.0; psi=0.2; omega=0.002; mu=0.0023;
epsilon=0.3;
gamma1=0.1; omega1=0.002; gamma2=0.3;
omega2=0.002; gamma3=0.75; omega3=0.002;
tspan=[0 500];
x0=[100000 33385 1311 65 54980 7911 319000
100000 33385 1311 65 54980 7911 319000 ...
100000 33385 1311 65 54980 7911 319000
100000 33385 1311 65 54980 7911 319000];
[t,x]=ode45(@corona_fekaduoverlab1,tspan,x0)
;
plot(t,x(:,3),t,x(:,10),t,x(:,17),t,x(:,24),'LineWid
h',2.5)
xlabel('Time(days)')
ylabel('Population')
title('Effects of \gamma on I_s')
legend('\gamma=0','\gamma=0.1','\gamma=0.3','
\gamma=0.75')
```

```
grid on
“.....”
“.....”
global Psi beta lamda q q1 gamma psi omega mu
epsilon ...
gamma1 omega1 gamma2 omega2 gamma3
omega3
Psi=500; beta=0.0004; lamda=0.006; q=0.0007;
q1=0.0003;
gamma=0.0; psi=0.2; omega=0.002; mu=0.0023;
epsilon=0.3;
gamma1=0.1; omega1=0.002; gamma2=0.3;
omega2=0.002; gamma3=0.75; omega3=0.002;
tspan=[0 500];
x0=[100000 33385 1311 65 54980 7911 319000
100000 33385 1311 65 54980 7911 319000 ...
100000 33385 1311 65 54980 7911 319000
100000 33385 1311 65 54980 7911 319000];
[t,x]=ode45(@corona_fekaduoverlab1,tspan,x0)
;
plot(t,x(:,3),t,x(:,10),t,x(:,17),t,x(:,24),'LineWid
h',2.5)
xlabel('Time(days)')
ylabel('Awarded infectious')
title('Effects of \gamma on I_a')
legend('\gamma=0','\gamma=0.1','\gamma=0.3','
\gamma=0.75')
```